Monitoring pH and solvent proticity with donor–acceptor-substituted biphenyls: a new approach towards highly sensitive and powerful fluorescent probes by tuning the molecular structure

Michael Maus*[a] and Knut Rurack[b]

[a] *Laboratory for Molecular Dynamics and Spectroscopy (MDS), Department of Chemistry, K.U. Leuven, Celestijnenlaan 200F, B-3001 Heverlee, Belgium. E-mail: Michael.Maus@chem.kuleuven.ac.be*

[b] *Federal Institute for Materials Research and Testing (BAM), Richard-Willstaetter Str. 11, D-12489 Berlin, Germany*

Received (in Cambridge, UK) 12th May 2000, Accepted 20th June 2000
Published on the Web 16th August 2000

The ability and structural requirements of 4-dimethylamino-4′-cyano-substituted biphenyls showing photoinduced intramolecular charge transfer (CT) to serve as hydrogen bond- or pH-sensitive fluorescent probes is investigated. The donor–acceptor (D–A) biphenyls **I** and **II** being planar in the CT excited state are most suitable as pH-sensitive fluorescent probes. The two compounds show analytically valuable features such as well-separated absorption and emission bands and signal changes spanning four orders of magnitude and can be employed in ratiometric, "self-calibrating", and highly sensitive pH fluorosensing in the range $0 < pH < 4$. Because of an enhanced charge separation in the excited state, the highly twisted D–A biphenyl **III** shows an increased proton sensitivity and can therefore be used to probe solvent proticity *via* hydrogen bond formation. The molecular and electronic characteristics of the two types of probes are discussed for the different neutral and acidic alcoholic and/or aqueous solvent mixtures investigated.

1. Introduction

In optical sensing applications, various methods such as absorption,[1] fluorescence (for reviews see ref. 2, 3) or phosphorescence[2d,4] spectroscopy are employed. In the field of spectroscopic pH monitoring, fluorescent pH indicators have been widely applied in recent years because fluorescence spectroscopy provides greater sensitivity (down to the single molecule level), has subnanometer spatial resolution, and is more convenient in many applications (*e.g.*, remote sensing with fiber optics) than the other non-invasive methods.[2,5] In analytical fluorometry, simple intensity measurements, lifetime sensing,[3,6–8] evanescent wave techniques,[9] as well as fluorescence correlation spectroscopy,[10] microscopy,[8,11] or flow cytometry[12] have been used. Depending on the sample of interest and the method of choice, the sensor molecules employed can be unbound or covalently linked to a supporting medium (*e.g.*, silica,[13] modified cellulose[14] or other polymers[6c,15]). Moreover, in the former case, the probe molecules can either be directly dissolved in the sample (tracer technique) or they can be embedded in various kinds of polymer matrices (organic polymers,[1a,16] sol–gels[1b,6b,9a,17]) or micro/nanoparticles.[18] Whereas the majority of publications on pH sensors deals with unifunctional fluorescent probes where the binding of a proton directly changes a photophysical property of the dye, binary systems comprising of a pH-sensitive proton receptor and a pH-insensitive reporter molecule are frequently encountered.[6d,7b,c,19] In both cases, often a pH-dependent long range intra- or inter-molecular charge/electron[3b,d,13,20,21] or energy[7b,c,22] transfer process is utilised for signalling. In order to overcome the usually limited dynamic sensing range (2–4 pH units), approaches were realised where two or more pH-sensitive probes with complementing pH responses are combined in a sensor array.[1d,7a,23] Only recently, multifunctional dye systems[24,25] or so-called AND/OR logic gates[26] opened new prospects in combined sensing applications which is especially of interest in biochemistry where simultaneous monitoring of analytes in, for instance, pH-driven ion transport is highly desired.[27,28b] Among the sensor molecules employed so far, fluorescein[6a,b,15,29,30] and anthracene[13,20a,21,26a,b] derivatives are mostly used† and only in some cases the intrinsic pH-sensitivity of autofluorescent biomolecules is utilised for sensing actions (*e.g.*, green fluorescent protein).[10,31] Concerning time-resolved fluorometry, the careful choice of a certain probe molecule allows one to choose a desired temporal (as well as spectral) sensing region in the pico- to milli-second time range.[6b,7b,c,19,32] On the basis of this great variety of probe molecules and possible sensor constitutions being available it is evident that fluorometric pH sensing can be applied in almost any liquid medium either with laboratory-based instrumentation or with remote sensors, fiber optic devices or so-called optodes.[2a–c,3a,19,30a,32,33a]

Besides sensitivity and selectivity, photostability is also a critical parameter in optical sensing applications. Here, approaches based on ratiometric sensing where analyte binding leads to the appearance of a new (well-separated) absorption or fluorescence band gained importance, since the intensity ratio of these two bands is independent of photo- or thermal-bleaching or changes of instrumental conditions such as optical path length, excitation intensity or detector sensitivity.[3d,6e,8,11,28,34] For fast ratiometric fluorosensing, the design of dyes showing dual emission (instead of ratio-able excitation bands) as a function of pH is highly desirable[24] but

† Other fluorophores include, *e.g.*, pyrene,[3d,36] lanthanide bound organic ligands,[6d,13,79] Ru(II) complexes,[6c,37,80] or various other dye systems.[2i,4b,20c–e]

practical examples are in a minority (as compared to systems showing dual excitation bands).[8b,25a,28b,30c,35] Moreover, many ratio-able sensor systems display extended response ranges as compared to single band systems. Unfortunately, some of these sensor molecules suffer from poorly separated emission bands.[30c,34b,c]

Besides the direct determination of protons, the indirect detection of many analytes such as CO_2,[7c,23b,c,33,36] ammonia[16,30d,37,38] or SO_2[39] *via* pH was realised. Depending on the problem encountered, fluorescent probes for extreme pH regions[1c,40] or for very narrow pH ranges[21a,37] (*e.g.*, in the acidic range for determining gaseous HCl or gastric acidity as well as for studying acidic organelles such as lysosomes—here, the most common probes of fluorescein– or aminoalkyl–anthracene-type cannot be employed) are required. Nowadays, the main fields of application include clinical analysis[7a,30d,36,41] and cellular biology[8,11,12,34,42] but fluorometric pH sensing is also found, for instance, in paper acidity estimation,[43] membrane[44] or environmental chemistry.[45] Furthermore, besides pH sensing in aqueous media the determination of pH in solvent mixtures or the detection of traces of water in organic solvents[46] and probing of solvent proticity (the ability to form hydrogen bonds)[15a,29,47,48] is an important analytical task.

As an extension of our work on charge transfer- (CT) and electron transfer (ET)-based fluorescent probes,[49,50] we have embarked on a study of dual emissive fluorescent pH indicators. In principle, any fluorescent dye molecule with protophilic functional groups which are part of or can interact with the fluorophore can display pH-dependent dual fluorescence. However, for dyes showing only a single emission band the observed shifts are usually comparatively small (see above). A more suitable approach is the utilisation of dyes which populate two (potentially) emissive states in the absence of protons, *i.e.*, which show dual fluorescence in aprotic solvents.[51] Here, donor–acceptor-substituted (D–A) biaryls have gained in importance during the past few years. For these dyes, radiative deactivation of the initially populated (locally excited) LE state has to compete with a fast intramolecular charge transfer (CT) reaction in the excited state to a second emissive species.[52,53b] Accordingly, for example, protonation at the donor in the ground state or hydrogen bonding interactions with the acceptor in the excited state can drastically alter absorption and/or fluorescence properties of such dyes. Since in solvents of high polarity some of these compounds show well-separated dual emission, advantageous in terms of sensitive and ratiometric sensing, several studies of the effect of pH on such a dual emission behaviour have been made recently.[49,54–57] Moreover, this design concept has been successfully introduced to metal ion sensing applications.[49,58]

In the present paper, we report on the proton-driven photophysics of donor–acceptor (D–A) biphenyls **I–III** (Scheme 1) containing a pH sensitive donor group (dimethylamino, DMA). Their interesting features for an application as fluorescent probes are based on an intramolecular charge transfer (CT) in the excited state within a few picoseconds.[53,59] During this CT process the electronic structure is changed from a more locally excited (^1L_b-type) state to a delocalized ^1CT (^1L_a-type) state and the structural relaxation is towards a planar

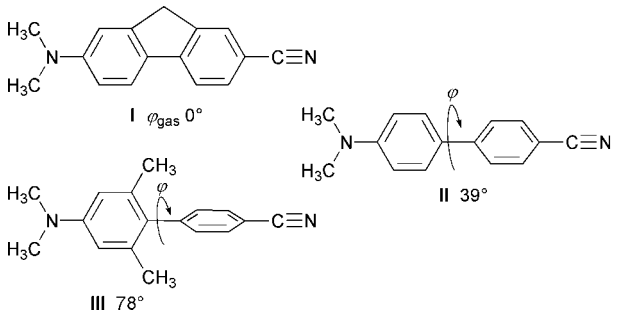

Scheme 1 Molecular structures of the investigated donor–acceptor (D–A) biphenyl fluorescent probes **I–III**. Calculated gas phase twist angles (φ) are also given.

conformation, a species denoted as **CT** in the text.[52,53,59,60] Only for **III** in medium and highly polar solvents, the initial relaxation towards a more planar conformation **CT** is followed by a viscosity-controlled rearrangement to a highly twisted species, labelled **CTR** in the text, with larger charge separation and, consequently, reduced fluorescence yields.[52,53,59,60]

The unusually high fluorescence quantum yields of the ^1CT states of **I–III** and the spectral separation of the ^1CT and ^1LE fluorescence and absorption bands render **I–III** as promising candidates for use as fluorescent pH probes. Besides studying potential applications in pH sensing, this contribution focuses on the electronic and structural (*e.g.*, the intramolecular twist angle φ) requirements of such compounds to serve as hydrogen bond and pH-sensitive fluorescent probes.

2. Results and discussion

2.1 Protic solvents

Fluorescence quenching mechanism in ethanol. Comparing the photophysical behaviour of **III** in ethanol (EtOH) at 298 K with that of **III** in acetonitrile (MeCN) as well as that of **I** and **II** in both highly polar protic and aprotic solvents, the high non-radiative rate constant (k_{nr}) of **III** in the protic solvent is apparent (Table 1). Considering that no indication for hydrogen bond formation in the ground state could be detected spectroscopically, the dynamic quenching process arises from a proton shift (PSh) from the solvent's hydroxyl group to the nitrilo group of **III** in the ^1CT excited state.[52] Omitting the deactivation to the ground state S_0 by internal conversion (IC), the basic mechanism involved is depicted in Scheme 2a. Whereas for **I** and **II**, the charge transfer excitation (CT) is followed by charge recombination (CR) fluorescence,‡ the proton shift and the subsequent non-radiative charge shift (CSh) is found only for **III**. Due to rapid transformation of the primarily populated **CT** species to the **CTR** species in highly polar ethanol, a twisted S_1 geometry with a reactive biradicaloid electronic structure ($D^{+\cdot}$–$A^{-\cdot}$) and a strongly localised negative charge density on the benzonitrile

‡ Detailed investigations[52,60] have revealed ultrafast additional electronic pathways to a ^1L_b/^1CT-type ^1LE (^1FC in ref. 60) state, which decays within a few picoseconds in aprotic solvents, but, as shown here, the lifetime of which can be increased in acidified solutions by partially supressing the charge transfer in S_1.

Table 1 Photophysical data of **I–III** in ethanol (EtOH) and acetonitrile (MeCN) at 298 K

	Solvent	$\tilde{\nu}_a/10^3$ cm^{-1}	$\tilde{\nu}_e/10^3$ cm^{-1}	Φ_f(%)	τ_f/ns	$k_f/10^7$ s^{-1}	$k_{nr}/10^7$ s^{-1}
I	EtOH	27.78	22.47	84	2.0	42	8
	MeCN	27.86	22.47	81	2.1	39	9
II	EtOH	28.99	21.93	81	2.2	37	9
	MeCN	29.07	21.79	79	2.2	35	10
III	EtOH	32.05	18.69	4	1.4	3	66
	MeCN	31.95	18.73	21	7.6	3	10

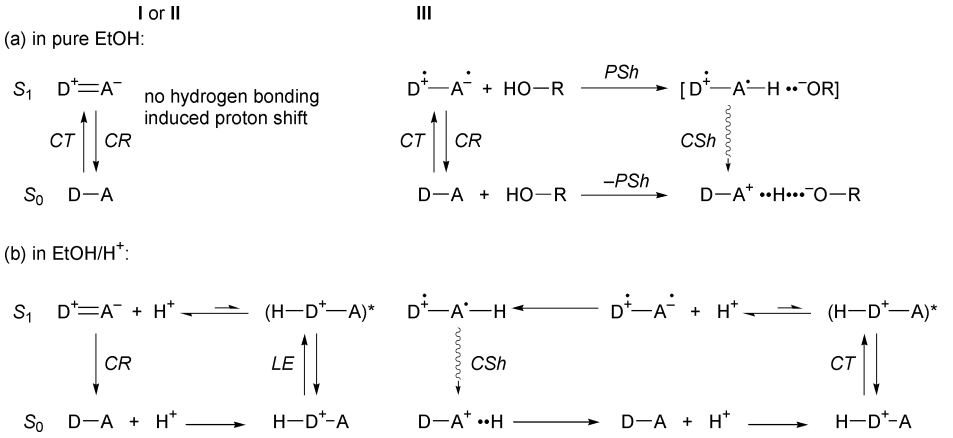

Scheme 2 Simple model for the photoinduced protonation cycles of **I**–**III** in (a) pure EtOH and (b) EtOH/H^+ (CT charge transfer excitation; CR charge recombination emission; CSh non-radiative intramolecular charge shift; PSh intermolecular proton shift; LE local excitation and emission of cyanobiphenyl chromophore, see text).

unit (A) is known to occur only in the case of the highly pretwisted D–A biphenyl **III**.[52]

Effect of temperature. The temperature-dependent photophysical properties of **I**–**III**, as shown in Fig. 1 for the overall fluorescence quantum yield $\Phi_f(T)$, the slow decay component $\tau_f(T)$, and the non-radiative rate constant $k_{nr}(T)$ (see eqn. (1)) of **III**, support the proposed Scheme 2.§

$$k_{nr}(T) = \frac{1 - \Phi_f(T)}{\tau_f(T)} \qquad k_f(T) = \frac{\Phi_f(T)}{\tau_f(T)} \tag{1}$$

In accordance with the simple photophysical model anticipated for **I** and **II** (Scheme 2a), *i.e.*, only a single **CT** species (D^+=A^-) emits, the fluorescence lifetimes of **I** and **II** remain constant (2.1 ± 0.1) ns over the temperature range 140–295 K

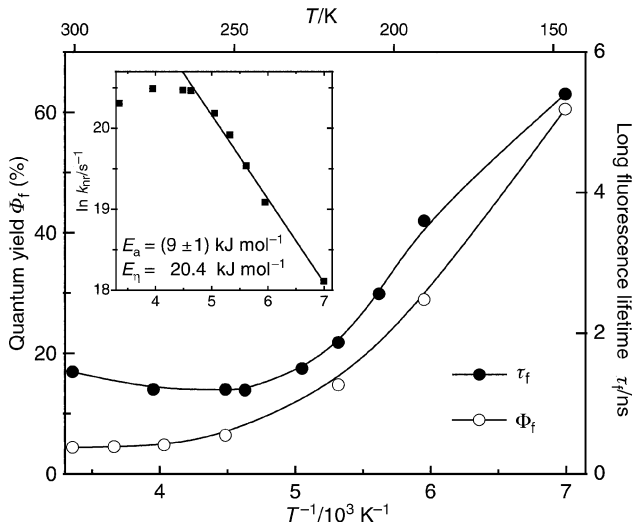

Fig. 1 Temperature dependence of the fluorescence lifetime (τ_f) and quantum yield (Φ_f) of **III** in ethanol. The Arrhenius plot of the corresponding non-radiative rate constants ($k_{nr} = (1 - \Phi_f)/\tau_f$) is shown in the inset. The derived Arrhenius barrier (E_a) and the activation energy for the viscous flow of the solvent (E_η) are also included.

§ Since in the polar solvent EtOH the adiabatic photoreaction CT → CTR occurs in the irreversible regime the long lifetime directly represents the intrinsic lifetime of the **CTR** species τ_f^0(CTR). However at low temperatures, $\Phi_f = x_{CT}\Phi_f^{CT} + x_{CTR}\Phi_f^{CTR}$ (with $x_i = c_i/\Sigma c_i$) slightly increases due to a larger contribution of Φ_f^{CT} and thus, correction of Φ_f with respect to the contribution of Φ_f^{CT} would decrease $k_{nr}(T)$ entailing an increase in activation barrier. Accordingly, the interpretation in the text is not affected by neglecting Φ_f^{CT} but would rather be supported by such a correction.

(not shown).¶ The almost parallel plots of Φ_f and τ_f for **III** in EtOH indicate only a moderately temperature-dependent fluorescence rate constant $k_f(T)$ (eqn. (1)) ranging from 3×10^7 s^{-1} at 298 K to 11×10^7 s^{-1} at 130 K, which is most probably due to the excited state equilibrium between the **CT** and the dominating **CTR** species in polar solvents. This S_1 equilibrium is slightly shifted towards the precursor **CT** species with lower temperatures/higher viscosities[52,53c,59] and therewith explains the somewhat larger k_f values at lower temperature. On the other hand, the increase in Φ_f and τ_f results from a freezing of the additional photochemical non-radiative channel (PSh in Scheme 2a). The Arrhenius barrier $E_a = 9$ kJ mol^{-1} as shown in the inset of Fig. 1 is approximately half that for the viscous flow of EtOH ($E_\eta = 20.4$ kJ) which is conceivable for a photoreaction inside a prearranged solvent cage. The temperature dependence of the photoreaction derives from both a less efficient formation of **CTR** from **CT** at lower temperatures and an energy barrier for the proton shift from EtOH to **CTR**. The deviation from the Arrhenius fit above 270 K can be explained with the acceleration of the back reaction from **CTR** to **CT** with respect to the forward reaction **CT** → **CTR**[52,59] such that less fluorescence is quenched. If the photoinduced proton shift is the active source of fluorescence quenching, this effect should be amplified by acidification of the solution. Thus, in the following section we will further address the proton affinity of excited **III** in the presence of an excess of protons.

Effect of added protons. In Fig. 2, the drastic change of the fluorescence emission and excitation spectra of **I**–**III** in acidic EtOH (0.3 M HCl and 10^{-5} M dye yielding a >10 000-fold excess of HCl) obviously reveals the strong influence of free (solvated) protons on the photophysics of all three donor–acceptor biphenyls. For example, dual fluorescence based on the excited state prototropic coexistence of the ^{1}CT and a locally excited (^{1}LE) state both representing the base (D^+=A^-) and the protonated (monocationic acid, (H–D^+–A)*) form is observed for **I** and **II** in EtOH/H^+ (Fig. 2). However, the emission spectrum of **III** lacks a CT band (explanation below). The proton-induced disappearance of the CT band in the fluorescence excitation as well as in the absorption spectra (not shown) of all the three dyes indicates that at the acid concentration employed only the protonated form exists in S_0

¶ A fast decay component τ_S, which however becomes rather slow at low temperatures (*e.g.* 1 ns at 168 K), is needed to fit the decays adequately. The well-known solvation probe coumarin 153 was simultaneously measured at 253 K and 168 K and showed exactly the same fast decay component. Along with the fact that the "normal" lifetimes τ_1 of **I** and **II** in EtOH are similar to those in diethyl ether this coincidence supports an attribution of τ_S to solvent relaxation processes (for temperature-dependent solvation times in ethanol, see ref. 81).

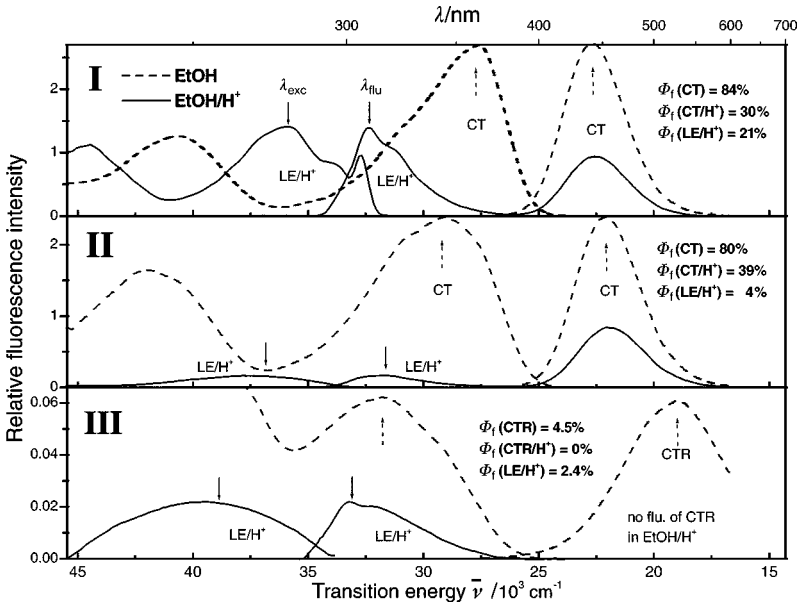

Fig. 2 Fluorescence emission and excitation spectra of **I–III** in EtOH prior to (– – –) and after (——) acidification at constant solute concentration. The optical densities at the CT absorption maximum were identical for **I–III** in EtOH (dashed arrow) and thus, all fluorescence intensities can directly be compared. The arrows indicate the excitation and emission wavelengths employed.

besides a very small amount of remaining unprotonated species as exemplified by a reduction of the CT absorption band to 1.5% (**II**), 0.75% (**I**), and <0.1% (**III**) of its initial intensity. Moreover, the blue-shifted first absorption band demonstrates that the proton is bound at the donor side (D), in particular occupying the free electron pair of the amino nitrogen atom. The molecular and electronic structures involved are discussed in the following section.

Since protonation of **I–III** takes place in the ground state where the equilibrium is strongly shifted towards the side of the protonated species, the CT fluorescence band arises after deprotonation in the excited state. This is corroborated by the calculation of pK_a^* employing eqn. (2).

$$pK_a^* - pK_a = \frac{\Delta G^* - \Delta G}{RT \ln 10} \quad (2)$$

where the acid–base (=LE/H^+–CT) free energy differences ΔG and ΔG^* in S_0 and S_1 can be derived from the Förster cycle[61] using the absorption and fluorescence energies (assuming a cancelling of entropy changes) yielding eqn. (3).

$$pK_a^* - pK_a = \frac{hc}{kT \ln 10}\left(\frac{\nu_a(CT) - \nu_f(CT)}{2} - \frac{\nu_a(LE/H^+) - \nu_f(LE/H^+)}{2}\right) \quad (3)$$

As an example for protonated solvents the resulting parameters of **I–III** in EtOH as well as in the EtOH/H_2O (1 : 1) mixture studied below are collected in Table 2. Taking into account the small pK_a values in the ground state (see next section), extremely negative pK_a^* values are obtained for the three D–A biphenyls pointing to a strong driving force ($\Delta G^* < 0$) for deprotonation in the excited state. Consequently, these experimental facts suggest that not only **I** and **II**, but also **III** is deprotonated in S_1 as well leading to the ^{1}CT state although its fluorescence is only observable in non-acidified EtOH. But for **III**, experiencing pronounced fluorescence quenching already in neutral EtOH (Table 1), this CT quenching process is even accelerated in EtOH/H^+. Accordingly, dynamic fluorescence quenching of **III** in EtOH/H^+ ($\Phi_f <$ 0.2%) is much stronger as compared to EtOH ($\Phi_f = 4.5\%$). Assuming a comparably fast ^{1}LE → ^{1}CT conversion for **III** as for **I** and **II**, where the deprotonation in S_1 partially recovers the CR fluorescence of the CT species (Fig. 2), recombination of the intermediately formed deprotonated CTR species $D^{+\cdot}$–$A^{-\cdot}$ of **III** with a proton from the environment efficiently occurs and quenches any CR fluorescence by rapid formation (PSh) of D^+–A–H followed by non-radiative decay (CSh) to the ground state of the latter (Scheme 2b, case of **III**). This reflects the higher proton activity in EtOH/H^+ rather than in pure EtOH and manifests the sensitivity of **III** towards proton and hydrogen bonding interactions. Furthermore, any quenching mechanism arising from bulk properties of the solvent was excluded by reference measurements in acetonitrile. Here, addition of small traces of EtOH leads to the expected reduction in fluorescence intensity in spite of the unchanged optical density supporting the mechanism of dynamic fluorescence quenching by a CSh mechanism as depicted in Scheme 2.

Table 2 $pK_a^* - pK_a$ Values for the prototropic equilibria of the LE/H^+ (acid) and CT (base) species of **I–III** determined by the Förster cycle (eqn. (3)) using the absorption ($\tilde{\nu}_a$) and fluorescence energies ($\tilde{\nu}_e$) of LE/H^+ and CT in protonated solvents

		$\tilde{\nu}_a/10^3$ cm^{-1}			$\tilde{\nu}_e/10^3$ cm^{-1}			$pK_a^* - pK_a$		
Solvent	Band	**I**	**II**	**III**	**I**	**II**	**III**	**I**	**II**	**III**
EtOH	LE/H^+	32.8[a]	37.8	39.4[b]	32.4[a]	31.6	33.2	−16	−19	−23
	CT	27.8	28.9	32.0	22.5	21.9	18.7[c]			
EtOH/H_2O (1 : 1)	LE/H^+	32.8[a]	37.7	[d]	32.4[a]	31.5	[d]	−17	−20	[d]
	CT	27.7	28.8	[d]	21.6	20.9	[d]			

[a] 0–0 energy. [b] From fluorescence excitation spectra. [c] Emission of CTR species. [d] Not determined.

From an applicational point of view, this behaviour distinguishes **III** as a very sensitive fluorescent probe for detecting the presence of protic solvents, *i.e.*, the fluorescence intensity of **III** can be utilised to monitor traces of, for instance, alcohols or water which were formed in a chemical reaction or condensation process in an aprotic medium. Practical applications would be based on a Stern–Vollmer-type calibration procedure, measuring the fluorescence intensity of **III** as a function of the concentration of the protic analyte in the liquid sample of interest.

2.2 Prototropic equilibria and pH-dependent dual absorption and emission

The basic emission features of **I–III** in acidic ethanol as summarized in Fig. 2 indicate the possibility of using the D–A biphenyls **I** and **II** as dual emissive, ratio-able fluorescent pH probes. Thus, in order to test the potential of these two compounds for possible applications, the pH-dependent studies were carried out in an ethanol/water 1 : 1 mixture, an aqueous solution for which HCl, employed for acidification, is known to have comparatively high mean activity coefficients ($\gamma_{\pm} \geqslant 0.68$ for pH > 1.4).[62] Here, probing pH in the range 2–5, in the region of the ground state pK_a of aromatic amines,[62–64] seems to be very promising. In this section, we demonstrate the suitability of both **I** and **II** for either absorption or fluorescence-based pH sensing and investigate the electronic and molecular structure involved before devoting our attention to sensing applications in the next section.

Determination of pK_a with absorption and fluorescence spectroscopy. The spectrophotometric and fluorometric pH titration spectra of **I** and **II** are shown in Fig. 3 and 4, the corresponding titration curves being included as insets. As can be deduced from these figures, both the CT absorption and fluorescence are enhanced with increasing pH and the opposite effect, *i.e.*, a decrease of both bands is observed upon proton addition. The reverse behaviour is found for the LE/H$^+$ bands. The isosbestic points in absorption centered at 255 nm and 308 nm for **I** and at 245 nm and 292 nm for **II** reflect the ground state acid–base equilibrium involving two species, *i.e.*, protonated H–D$^+$–A responsible for the LE/H$^+$ bands and neutral D–A responsible for the CT bands. From the inflection points of the LE/H$^+$ and CT spectrophotometric titration curves shown in the insets of Fig. 3, the ground state pK_a values are determined to be 2.45 for **I** and 2.35 for **II**, independently of the band monitored. This value is somewhat lower than that of various aromatic amines (*cf.* pK_a = 4.5 for aniline)[63] but is in good agreement with values reported for other anilino derivatives carrying an electron withdrawing substituent (*e.g.*, pK_a = 2.5 for *para*-anthracen-9-yldimethylaniline ADMA in ethanol/water 4 : 1,[64] pK_a = 3.30 for *para*-(8-boradipyrromethenyl)dimethylaniline in methanol/water 1 : 1,[56b] pK_a = 3.38 for 9-*para*-dimethylanilino-10-methylacridinium perchlorate in water[65]), comparable to the benzonitrile acceptor moiety of **I** and **II**.

The insets of Fig. 4 showing the fluorometric titration spectra reveal that a fluorescence titration performed by exciting at the maximum of either the LE/H$^+$ or the CT absorption band yields very similar pK_a. Accordingly, both the spectrophotometric and fluorometric titrations yield a slightly smaller pK_a for **II** as compared to **I**, most probably arising from a stronger π-delocalisation of the lone electron pair of the dimethylamino nitrogen atom in **II**.

Assignments of absorption and emission. The low energy absorption and fluorescence emanates from the S_0–^{1}CT electronic transition which is reflected by a pronounced bathochromic shift in emission upon increasing the solvent polarity

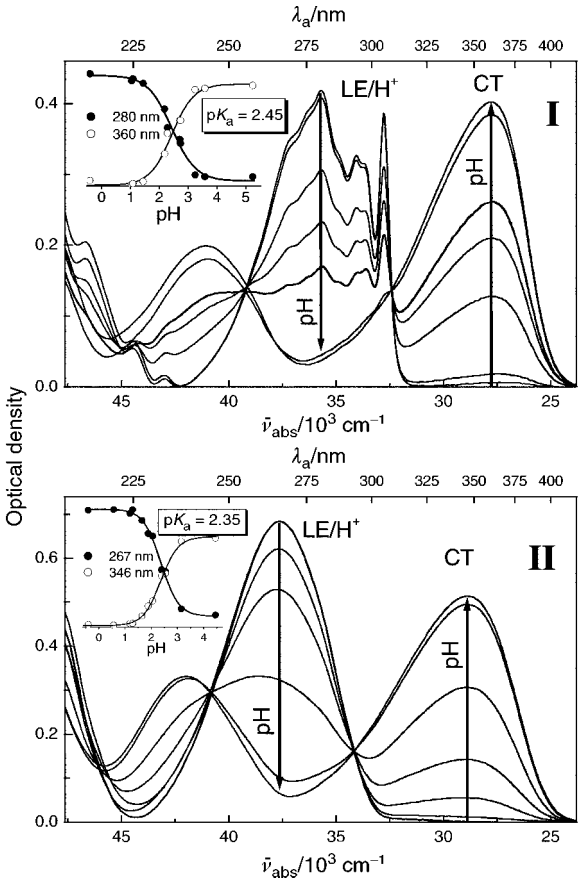

Fig. 3 pH-dependent absorption spectra and titration curves of **I** and **II** in EtOH/H_2O 1 : 1 (v/v). For pH titration steps, see Fig. 4.

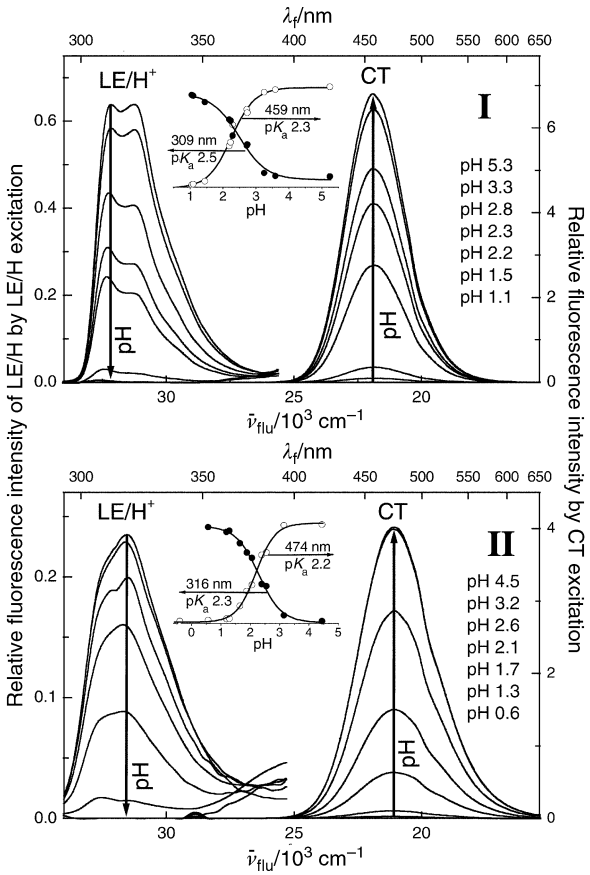

Fig. 4 pH-dependent fluorescence spectra and titration curves of **I** and **II** in EtOH/H_2O 1 : 1 (v/v). The pH titration steps are indicated.

from EtOH to EtOH/H_2O (Table 2). The absence of a hypsochromic shift in absorption excludes hydrogen bond formation between the electron-donating DMA group and added water molecules in the ground state. On the other hand, the LE/H^+ absorption spectra of **I** and **II** presented in Fig. 3 are different with respect to band position and structure and, besides indicating different electronic characteristics of both molecules, contain a wealth of important information. Comparison of the LE/H^+ absorption maximum of **II** ($\tilde{\nu}_a$ = 37 800 cm^{-1}) with the $S_0 \rightarrow {}^1L_a$ maxima of unsubstituted biphenyl ($\tilde{\nu}_a$ = 39 700 cm^{-1}),[66] *para*-dimethylaminobiphenyl ($\tilde{\nu}_a$ = 33 900 cm^{-1}),[67] and *para*-cyanobiphenyl ($\tilde{\nu}_a$ = 37 500 cm^{-1})[68] identifies the cyanobiphenyl entity in **II** as being responsible for absorbing the main photon energy in **II**. This can be directly related to the complete withdrawal of the lone electron pair of the amino nitrogen atom from the π-electron system upon its protonation. In the case of **I**, the shape of the structured absorption band differs from that of the parent, unsubstituted fluorene[66] in two ways: (i) the global maximum is not the sharp 0–0 band at 32 800 cm^{-1} (33 100 cm^{-1} in unsubstituted fluorene) but the vibronic band at 35 700 cm^{-1} and (ii) the ^1L_a band of fluorene at 40 000 cm^{-1} is not visible in **I**. Thus, it can be deduced that the ^1L_a band of the parent fluorene is red-shifted in **I** appearing at nearly the same spectral position as the ^1L_a band in **II**. Hence, both bands, the unstructured ^1L_a and the structured ^1L_b band of **I**, strongly overlap. Similar to the behaviour of the pair of parent biphenyls,[66] only the ^1L_b absorption band of the fluorene D–A derivative is strongly intense.[69] Moreover, note that the good agreement of the 0–0 band of **I** in EtOH/H_2O (32 800 cm^{-1}) with the minimum of the second derivative $\varepsilon''(\nu_a)$ spectrum of **I** in acetonitrile (33 200 cm^{-1})[69] proves that the previous assignment of the hidden structure to the ^1L_b transition is correct.[69] This means that LE/H^+ emission occurs from the ^1L_b-type state in both cases, **I** and **II**. Assuming similar rates for LE/H^+–CT conversion in **III** (see below), the distinctly smaller fluorescence quantum yields of **II** (Φ_f(LE/H^+) = 4%) and **III** (Φ_f(LE/H^+) = 2.4%) as compared to **I** (Φ_f(LE/H^+) = 21%) in acidic ethanol are consistent with emission from ^1L_b, which is strong only for **I** because of symmetry reasons.[52,69]

Based on the experimental results given above, a refined reaction cycle assumed to govern the prototropic equilibria of **I** and **II** is illustrated in Scheme 3. For better clarity, only the general term "LE" is used for local ^1L_a- or ^1L_b-type absorption and local ^1L_b-type emission in Scheme 3.

Slow prototropic equilibrium in S_1. The occurrence of dual fluorescence of the acid and base species over a large pH range (Fig. 3 to 5) as well as the similarity of the spectrophotometric and fluorometric titration curves with inflection points at nearly identical pK_a point to a slow prototropic equilibrium in S_1 where the radiative deactivation successfully competes with the proton transfer (dissociation) processes. However, an explanation for the apparent discrepancy between a slow excited state dissociation reaction and strongly negative pK_a^*, *i.e.*, a strong thermodynamic driving force for the acid-to-base or LE/H^+-to-CT deprotonation, has yet to be given. Whereas the lack of LE/H^+ emission after pure CT excitation is conceivable with a too endergonic base-to-acid (CT-to-LE/H^+) reaction, the slow acid-to-base (LE/H^+-to-CT) reaction contradicts the considerably negative free enthalpy change derived from the Förster cycle (Table 2). However, we can gain access to an explanation for this phenomenon by considering an excited state reaction scheme which does not involve direct LE/H^+–CT interconversion but an intermediate deprotonated LE species as depicted in Scheme 3. The release of the proton extends the π-electron delocalisation from the *para*-cyanobiphenyl unit to the whole chromophoric π-system, the electronic structure of which has been characterised by a mixing of ^1L_b(A)- and ^1L_b(D)-type configurations in a previous study.[69] But despite increased π-electron delocalisation, the remaining ^1L_b electronic nature (in the case of ^1L_a absorption, IC from ^1L_a to ^1L_b occurs first within a few femtoseconds) allows only a weak energetic stabilisation resulting in a comparatively slow LE/$H^+ \rightarrow$ LE process. Note again the similarity between the 0–0 energy for the $S_0 \rightarrow {}^1L_b$ absorption of the protonated form (Fig. 3) and the free base (as derived from the h_2 band in Fig. 3 of ref. 69) explaining the small driving force. Interestingly, slow LE/$H^+ \rightarrow$ LE deprotonation reactions have also been reported for the charge transfer processing biaryls 1-(*para*-aminophenyl)-pyrene and ADMA.[62,64]

In comparison to the deprotonation reaction, the subsequent electron transfer (ET) to the CT species is quite rapid due to strong exergonicity. The latter process is reminiscent of the excited state electron transfer $^1FC \rightarrow {}^1CT$ interconversion observed by time-resolved transient absorption for **I** and **II**.[60] Correspondingly, the LE species populated by excited state deprotonation (Scheme 3) is equivalent to the species populated after vibrational Franck–Condon relaxation as observed in the transient absorption study.[60] Thus, both pH-dependent fluorescence and time-resolved transient absorption[60] experiments agree in identifying the primarily populated excited state species as an independent and stable electronic state. Future time-resolved transient absorption investigations in acidified solutions should therefore reveal a delay of the electron transfer step in S_1.

Dynamic quenching of CT fluorescence in I and II. Fig. 5 shows that the logarithmic intensity ratio of CT-to-LE/H^+ fluorescence linearly decreases with increasing acid concentration down to pH ≈ 1. The data point recorded under much stronger acidic conditions (pH ≈ −0.4) clearly deviates from the fit, indicating a weaker CT fluorescence as would be expected from an extrapolation of the data obtained at pH > 0.8. This indicates that the unprotonated CT species experiences a quenching process which is most probably induced by the same mechanism observed before for **III** in acidic EtOH (Fig. 2, see above). Accordingly, at this high proton concentration quenching of a biradicaloid $D^{+\cdot}$–$A^{-\cdot}$ species can be attributed to protonation of the partially negatively charged nitrilo acceptor group (Scheme 3). Moreover, the fluorescence intensity ratio I_f(CT)/I_f(LE/H^+) < 0.3 suggests that in the above described experiments in EtOH/H^+, where ratios of 0.7 (**I**) and 5.1 (**II**) were found (Fig. 2), a higher pH > 0 of the solution can be expected. (Note that the exact pH of that solution was not measured, but the 14-times smaller HCl concentration and the smaller proton activity coefficients support the observation of less effective proton-induced quenching at a pH > 0.)

2.3 Sensitive and ratiometric sensing of pH

Pursuing a ratiometric, "self-calibrating",‖ easy-to-measure and highly sensitive fluorometric method to probe pH, the biphenyls **I** and **II** can be employed in combination with a simple dual excitation/dual emission technique. Here, the ratio of CT-to-LE fluorescence $I_{ex}I_{flu}$(CT)/$I_{ex}I_{flu}$(LE/H^+) as obtained by measuring LE/H^+-excited (at the absorption maximum), LE/H^+ emission (at the emission maximum) and CT-excited CT emission (*cf.* Fig. 3 and 4) is used to quantify the proton concentration in solution. The superiority of this ratiometric method, which is more advanced as compared to the commonly employed measurement of fluorescence

‖ The term "self-calibrating" refers to the insensitivity of this dual excitation/dual emission technique towards changes of instrumental parameters as discussed in the Introduction. Fluctuations of the light source or variations of the optical path length require no recalibration.

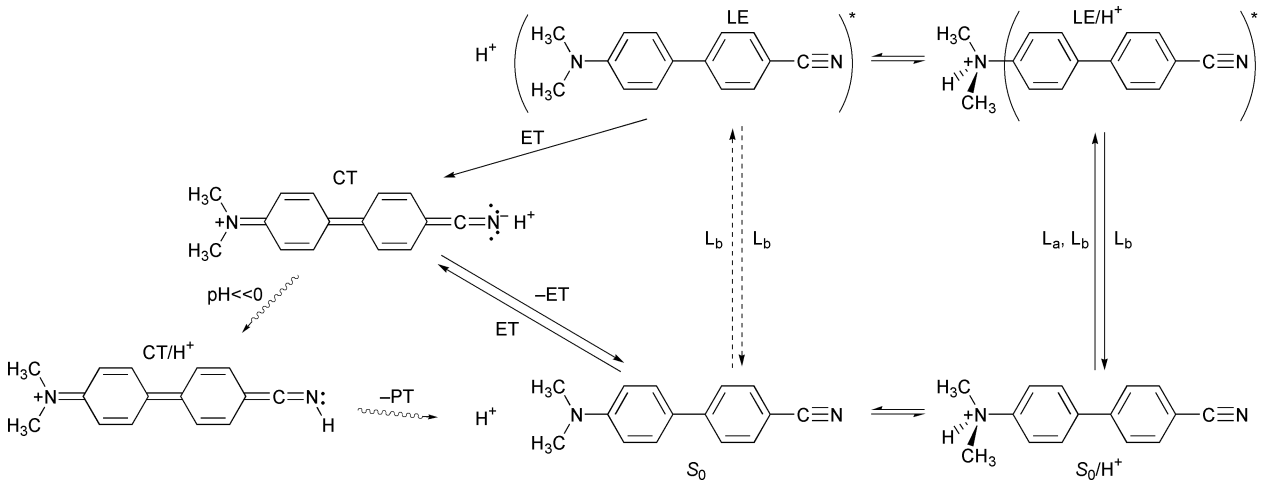

Scheme 3 Refined prototropic reaction cycle for **II** (and **I**) showing the electronic structures and transitions which account for the observed spectroscopic behaviour (L_b, L_a electronic absorption and emission transitions according to Platt nomenclature;[82] ET, −ET electronic transition with strong electron transfer character; PT, −PT proton transfer between solute and solvent).

enhancement or quenching with excitation at a single wavelength, *i.e.*, the isosbestic point,[5,24] is presented in this section.

The basic requirements for ratiometric fluorescence sensing, *i.e.*, well-separated absorption and fluorescence bands to allow an optimum independence of detector sensitivity or probe concentration and minimum interference due to excitation of both ground state species, are met by the biphenyls **I** and **II**. The absence of wavelength shifts is also an advantageous feature of these sensor molecules. Furthermore, the comparatively large dynamic sensing range of 4 pH units and the linear calibration curves (with correlation coefficients >0.99), which directly follow from Fig. 6, are of high analytical value.

A more elaborate requirement, *i.e.*, highly sensitive quantitative detection of *both* signalling species of the probe molecule, acid *and* base form, is usually hardest to meet but again, Fig. 6 demonstrates the enormous potential of **I** and **II** as exemplified by a signal change covering four orders of magnitude (ratios between 0.1 and 1000). Such large variations can only be achieved by a combination of drastic changes in both absorption *and* fluorescence intensity of separated bands and are scarcely found for systems where only the ratio of fluorescence intensity is considered (with excitation at an isosbestic point or detection at an isoemissive point).[8b,25a,28b,30c,35] In accordance with the prototropic photophysical behaviour outlined above, the calibration curve for **II** is higher lying than that for **I** because the intrinsic fluorescence yield from LE/H$^+$ is lower for **II** (short-axis polarised ^1L_b fluorescence with small k_f) than for **I** (the fluorene derivative with long-axis polarised ^1L_b fluorescence and large k_f).

Further advantages of **I** and **II** are the large extinction coefficients for the base as well as for the acid form (ε_{max}(**I**) ≈ 4 × 10^4 M^{-1} cm^{-1}, ε_{max}(**II**) ≈ 3 × 10^4 M^{-1} cm^{-1}) and the sizeable fluorescence quantum yields of both excited state species. (Note that the often encountered problem of proton-induced quenching of CT fluorescence is absent for **I** and **II** at pH > 0.5.) Especially for **I**, ε_{max} as well as Φ_f of the pure base (CT) and acid (LE/H$^+$) form are comparatively large (Fig. 2 to 4).

All these various favourable features can be traced back to the specific electronic and conformational properties of **I** and **II**. (i) The zero–order electron transfer state of **I** and **II** in polar solvents like water is considerably lower lying than the next locally excited state. Such a situation is difficult to achieve in biaryls with larger polycyclic aromatic subunits like anthracence or pyrene showing completely overlapping CT and LE absorption bands.[62,64,70] Thus, the complete separation of fluorescence *and* (!) absorption bands are, to the best of our knowledge, unique features of the present dyes enabling an elegant measurement of the ratio between LE/H$^+$-excited LE/H$^+$ fluorescence and CT-excited CT fluorescence. (ii) The planar conformation of **I** and **II** in the ^{1}CT state is responsible

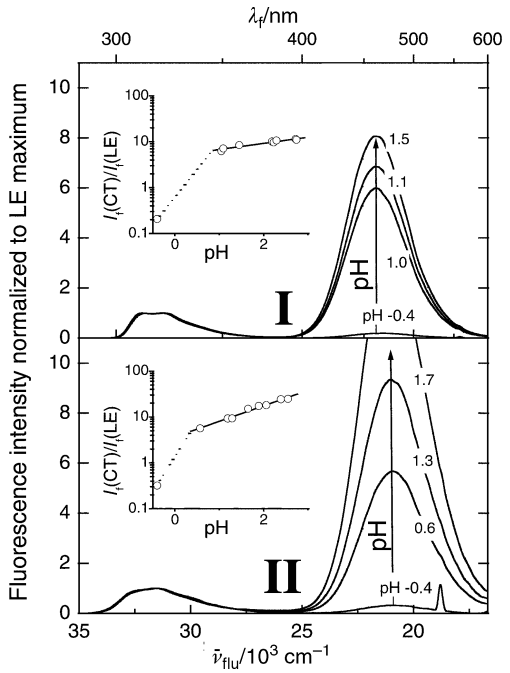

Fig. 5 Normalised (on the LE/H$^+$ band) fluorescence spectra of **I** and **II** in EtOH/H_2O/H$^+$ at pH < pK_a obtained by excitation at the LE/H$^+$ absorption maximum. The plot of the intensity ratios in the inset deviates from linearity at pH < 1.

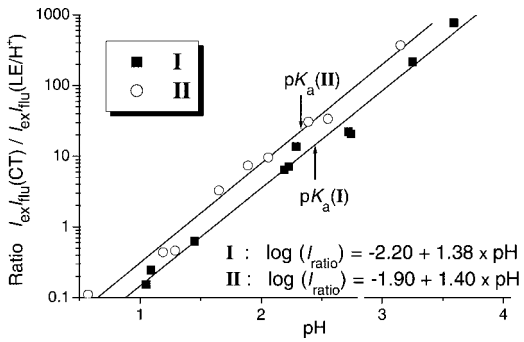

Fig. 6 pH calibration curves using the fluorescence intensity ratio between CT-excited CT emission and LE/H$^+$-excited LE/H$^+$ emission. The correlation coefficients of both linear fits are r = 0.993.

for an appreciable HOMO–LUMO overlap associated with unusally large S_0–CT electronic transition moments.[59,69,71] Accordingly, high absorption and fluorescence intensities and the delocalised electronic structure of CT add to the above mentioned advantages.

3. Conclusion

Photoinduced intramolecular charge transfer in donor–acceptor (D–A) biphenyls was shown to be very useful in sensing hydrogen bonds as well as protons. The molecular design of the probe compounds, which was varied in these studies by the twist angle φ between donor and acceptor moiety, determines which specific microenvironmental property can be probed.

The D–A biaryls **I** and **II** are planar in the ^{1}CT excited state with a delocalized $\pi\pi^*$-electronic structure and show very promising pH sensing properties, because formation of the protonated forms **I**–H$^+$ and **II**–H$^+$ on the timescale of the fluorescence lifetime leads to dual fluorescence and absorption of the ^{1}CT and locally excited (^{1}LE) states.

In contrast, **III** exists in a highly twisted conformation with localised charges on both phenyl subunits in the $S_1(^1\text{CT})$ state giving rise to strong specific interactions with potential quenchers such as protic solvents and protons as a consequence of an attack at the charged atomic centers. Hence, the fluorescence from ^{1}CT of **III** is efficiently quenched in acidic solutions so that only the ^{1}LE fluorescence can be observed. This high sensitivity of **III** can thus be employed to monitor solvent proticity.

The occurrence of dual, LE and CT, fluorescence of **I** and **II** at a pH close to the pK_a of $\approx$2.4 reflects a slow prototropic equilibrium between the LE/H$^+$ acid form and the CT basic form. Because the direct conversion from LE/H$^+$ to CT would be highly exergonic, this behaviour can only be explained by the involvement of an intermediate LE basic form which rapidly reacts to give the CT base. Intramolecular twisting or highly acidic conditions open an additional non-emissive channel, which we assign to the formation of a positively charged CT/H$^+$ electronic structure resembling cationic biphenyls that are known to undergo a photoinduced highly efficient non-radiative intramolecular charge shift.[72,73]

In conclusion, we have shown that molecular engineering of D–A biaryls by tuning the twist angle between donor and acceptor and by careful consideration of donor/acceptor energetics determining the energy gap between LE and CT states can yield very sensitive and powerful fluorescent probes showing either well-separated, ratio-able, intense LE and CT absorption and fluorescence bands (**I** and **II**) or very hydrogen bond-sensitive quenching of CT emission (**III**).

4. Experimental

4.1. Materials

The synthesis of compounds **I**–**III** is described elsewhere.[52] Ethanol and acetonitrile of UV spectroscopic grade, hydrochloric acid (10 M; 37% by weight HCl) purchased from Merck, respectively, and doubly distilled water were used.

4.2. Steady-state absorption and fluorescence spectroscopy

Steady-state measurements were performed on an ATI UNICAM UV4 spectrophotometer and an Aminco Bowman 2 fluorometer with 2 nm band passes. Fluorescence spectra were corrected for detector response and time-drift and were additionally converted from the recorded wavelength scale $I_f(\lambda_f)$ to a linear energy scale according to $I_f(\nu_f) = I_f(\lambda_f) \times \lambda_f^2$. The fluorescence quantum yields (Φ_f) were determined relative to quinine sulfate dihydrate (NIST standard reference material SRM no. 936) in 0.5 M H_2SO_4 ($\Phi_f = 0.52$)[74] at optical densities less than 0.1.[75]

4.3 Fluorescence decay times

The time-resolved fluorescence measurements were performed with synchrotron radiation from the Berlin Storage Ring for Synchrotron Radiation (BESSY) using a time-correlated single photon counting setup described in more detail elsewhere.[52] The temporal calibration of the experimental setup for the time-resolved measurements was checked with 1,4-bis(5-phenyloxazol-2-yl)benzene (POPOP) in ethanol ($\tau_f = 1.35$ ns $\pm$ 0.20 ns),[76] and fluorescein 27 in 0.1 M NaOH ($\tau_f = 4.50$ ns $\pm$ 0.03 ns).[76] The decay analysis using the least-squares and iterative deconvolution method implemented in the PC program Global Unlimited V2.2 (LFDG, University of Illinois) allowed a temporal resolution of less than 200 ps. The goodness of the decay fits were judged by reduced chi-squared ($\chi^2_R < 1.2$), the residuals and the autocorrelation function $C(j)$ of the residuals.

4.4. Temperature-dependent measurements

Temperature-dependent fluorescence was measured with a home-made cooling apparatus which allows one to freeze and control the temperature of four samples in quartz cuvettes by pumping cold nitrogen gas through the cryostat. The temperature precision and stability decreases with cooling and is $< \pm 1$ K down to 185 K. The optical densities at low temperatures required for the calculation of the fluorescence quantum yields ($\Phi_f(T)$) were derived relative to the room temperature data by correcting for the change of the refractive index, density[77] and the absorption band shape.[59] The absolute error of $\Phi_f(T)$ determined from the integrated intensity area relative to the values at room temperature is less than 10%.

4.5. Measurements of pH

For every step of the pH titration, small amounts of 10 M (37% by weight) HCl were added (microliter pipette, Eppendorf) to 50 mL of a solution containing 1.1×10^{-5} M of **I** or 2.0×10^{-5} M of **II** in an ethanol–water mixture (1 : 1 v/v). After stirring for 3 min, 3 mL of the solution were transferred to a 10 mm quartz cuvette and additionally stirred for 1 min. The pH was monitored using a digital pH meter (WTW pH 537) equipped with a glass electrode (Mettler Toledo InLab 423). Only in the case of the highly acidic solution (pH = -0.44) was a fresh sample prepared (see below). Calibration of the instrument was performed with standard aqueous solutions of pH = 1.68, 4.01, 6.86 and 9.18 from WTW. The measured value (pH^{mes}) was corrected by taking into account differences in liquid junction potentials (ΔU_j) and proton activity coefficients ($\Delta\log\gamma_{H^+}$) between the solvent mixture of the sample and the aqueous calibration solution according to eqn. (4).[78]

$$\text{pH} = \text{pH}^{mes} - \Delta U_j + \Delta \log \gamma_{H^+} = \text{pH}^{mes} - 0.21 \qquad (4)$$

From multiple titrations ($N = 4$), the error of pH^{mes} in the range of $1 < \text{pH} < 6$ was determined to $\leqslant$0.2 pH units. The pH value of the highly acidic sample was directly calculated from the analytical acid concentration in the mixture of 5 mL EtOH, 2.75 mL 10 M HCl, and 2.25 mL H_2O to be -0.44 without correction for the activity coefficient ($\gamma_\pm$). Since $\gamma_\pm$ amounts to 0.7 for the relevant EtOH/H_2O (1 : 1) mixture in a concentration range of 0.05 M to 0.1 M HCl,[62] the value used here can be regarded as a lower limit. A more realistic value close to zero would strengthen the interpretation in the text,

i.e., proton-induced CT quenching occurs for pH < 1 (*cf.* Fig. 5).

Acknowledgements

We thank Professor W. Rettig and the Deutsche Forschungsgemeinschaft for financial support (DFG Re 387/9-1, Re 387/9-2, Re 387/8-2) during the experimental part of the present work.

References

1 (*a*) J. I. Peterson, S. R. Goldstein, R. V. Fitzgerald and D. K. Buckhold, *Anal. Chem.*, 1980, **52**, 864; (*b*) V. Chernyak, R. Reisfeld, R. Gvishi and D. Venezky, *Sens. Mater.*, 1990, **2**, 117; (*c*) A. Safavi and H. Abdollahi, *Anal. Chim. Acta*, 1998, **367**, 167; (*d*) H. Hisamoto, H. Tohma, T. Yamada, K.-I. Yamauchi, D. Siswanta, N. Yoshioka and K. Suzuki, *Anal. Chim. Acta*, 1998, **373**, 271.

2 (*a*) J. I. Peterson and G. G. Vurek, *Science*, 1984, **224**, 123; (*b*) W. R. Seitz, *Anal. Chem.*, 1984, **56**, 16A; (*c*) L. W. Burgess, M.-R. S. Fuh and G. Christian, in *Progress in Analytical Luminescence*, eds. D. Eastwood and L. J. C. Love, ASTM, Philadelphia, 1988, p. 100; (*d*) E. L. Wehry, in *Practical Fluorescence*, ed. G. G. Guilbault, Marcel Dekker, New York, 2nd edn., 1990, p. 75; (*e*) A. Sharma, *Proc. SPIE-Int. Soc. Opt. Eng.*, 1992, **1637**, 270; (*f*) B. Valeur, in *Molecular Luminescence Spectroscopy*, ed. S. G. Schulman, J. Wiley & Sons, New York, 1993, vol. 3, p. 25; (*g*) *Probe Design and Chemical Sensing*, ed. J. R. Lakowicz, Plenum, New York, 1994; (*h*) *Fluorescent Probes in Cellular and Molecular Biology*, ed. J. Slavik, CRC, Boca Raton, FL, 1994; (*i*) A. P. de Silva, H. Q. N. Gunaratne, T. Gunnlaugsson, A. J. M. Huxley, C. P. McCoy, J. T. Rademacher and T. E. Rice, *Chem. Rev.*, 1997, **97**, 1515.

3 (*a*) M. E. Lippitsch and S. Draxler, *Sens. Actuators B*, 1993, **11**, 97; (*b*) S. Draxler and M. E. Lippitsch, *Sens. Actuators B*, 1995, **29**, 199; (*c*) S. Draxler and M. E. Lippitsch, *Appl. Opt.*, 1996, **35**, 4117; (*d*) M. E. Lippitsch, D. Kieslinger and S. Draxler, *Sens. Actuators B*, 1997, **38–39**, 96.

4 (*a*) R. A. Bissell and A. P. de Silva, *J. Chem. Soc., Chem. Commun.*, 1991, 1148; (*b*) D. B. Papkovsky, G. V. Ponomarev and O. S. Wolfbeis, *Spectrochim. Acta, Part A*, 1996, **52**, 1629.

5 W. Rettig and R. Lapouyade, in *Probe Design and Chemical Sensing*, ed. J. R. Lakowicz, Plenum, New York, 1994, p. 109.

6 (*a*) H. Szmacinski and J. R. Lakowicz, *Anal. Chem.*, 1993, **65**, 1668; (*b*) C. A. Browne, D. H. Tarrant, M. S. Otteanu, J. W. Mullens and E. L. Chronister, *Anal. Chem.*, 1996, **68**, 2289; (*c*) J. M. Price, W. Xu, J. N. Demas and B. A. DeGraff, *Anal. Chem.*, 1998, **70**, 265; (*d*) M. A. Kessler, *Anal. Chem.*, 1999, **71**, 1540; (*e*) H.-J. Lin, H. Szmacinski and J. R. Lakowicz, *Anal. Biochem.*, 1999, **269**, 162.

7 (*a*) O. S. Wolfbeis, I. Klimant, T. Werner, C. Huber, U. Kosch, C. Krause, G. Neurauter and A. Dürkop, *Sens. Actuators B*, 1998, **51**, 17; (*b*) U. Kosch, I. Klimant, T. Werner and O. S. Wolfbeis, *Anal. Chem.*, 1998, **70**, 3892; (*c*) G. Neurauter, I. Klimant and O. S. Wolfbeis, *Anal. Chim. Acta*, 1999, **382**, 67.

8 (*a*) R. Sanders, A. Draaijer, H. C. Gerritsen, P. M. Houpt and Y. K. Levine, *Anal. Biochem.*, 1995, **227**, 302; (*b*) A. Srivastava and G. Krishnamoorthy, *Anal. Biochem.*, 1997, **249**, 140.

9 (*a*) B. D. MacCraith, V. Ruddy, C. Potter, B. O'Kelly and J. F. McGilp, *Electron. Lett.*, 1991, **27**, 1247; (*b*) J. P. Golden, L. C. Shriver-Lake, G. P. Anderson, R. B. Thompson and F. S. Liger, *Opt. Eng.*, 1992, **31**, 1458.

10 J. Widengren, B. Terry and R. Rigler, *Chem. Phys.*, 1999, **249**, 259.

11 (*a*) K. W. Dunn, S. Mayor, J. N. Myers and F. R. Maxfield, *FASEB J.*, 1994, **8**, 573; (*b*) B. J. Muller-Borer, H. Yang, S. A. M. Marzouk, J. J. Lemasters and W. E. Cascio, *Am. J. Physiol.*, 1998, **275**, H1937.

12 I. Vergne, P. Constant and G. Laneelle, *Anal. Biochem.*, 1998, **255**, 127.

13 M. Ayadim, J.-L. Habib Jiwan, A. P. de Silva and J.-P. Soumillion, *Tetrahedron Lett.*, 1996, **37**, 7039.

14 O. S. Wolfbeis, N. V. Rodriguez and T. Werner, *Mikrochim. Acta*, 1992, **108**, 133.

15 (*a*) K. J. Shea, D. Y. Sasaki and G. J. Stoddard, *Macromolecules*, 1989, **22**, 1722; (*b*) D. Millar, M. Uttamlal, R. Henderson and A. Keeper, *Chem. Commun.*, 1998, 477.

16 O. S. Wolfbeis and H. E. Posch, *Anal. Chim. Acta*, 1986, **185**, 321.

17 (*a*) L. Yang and S. S. Saavedra, *Anal. Chem.*, 1995, **67**, 1307; (*b*) O. Ben-David, E. Shafir, I. Gilath, Y. Prior and D. Avnir, *Chem. Mater.*, 1997, **9**, 2255; (*c*) A. Lobnik, I. Oehme, I. Murkovic and O. S. Wolfbeis, *Anal. Chim. Acta*, 1998, **367**, 159.

18 (*a*) H. A. Clark, S. L. R. Barker, M. Brasuel, M. T. Miller, E. Monson, S. Parus, Z.-Y. Shi, A. Song, B. Thorsrud, R. Kopelman, A. Ade, W. Meixner, B. Athey, M. Hoyer, D. Hill, R. Lightle and M. A. Philbert, *Sens. Actuators B*, 1998, **51**, 12; (*b*) H. A. Clark, R. Kopelman, R. Tjalkens and M. A. Philbert, *Anal. Chem.*, 1999, **71**, 4837.

19 U. Kosch, I. Klimant and O. S. Wolfbeis, *Fresenius J. Anal. Chem.*, 1999, **364**, 48.

20 (*a*) A. P. de Silva and R. A. D. D. Rupasinghe, *J. Chem. Soc., Chem. Commun.*, 1985, 1669; (*b*) A. J. Bryan, A. P. de Silva, S. A. de Silva, R. A. D. D. Rupasinghe and K. R. A. S. Sandanayake, *Biosensors*, 1989, **4**, 169; (*c*) R. A. Bissell, E. Calle, A. P. de Silva, S. A. de Silva, H. Q. N. Gunaratne, J.-L. Habib Jiwan, S. L. A. Peiris, R. A. D. D. Rupasinghe, T. K. S. D. Samarasinghe, K. R. A. S. Sandanayake and J.-P. Soumillion, *J. Chem. Soc., Perkin Trans. 2*, 1992, 1559; (*d*) A. P. de Silva, H. Q. N. Gunaratne, P. L. M. Lynch, A. J. Patty and G. L. Spence, *J. Chem. Soc., Perkin Trans. 2*, 1993, 1611; (*e*) L. M. Daffy, A. P. de Silva, H. Q. N. Gunaratne, C. Huber, P. L. M. Lynch, T. Werner and O. S. Wolfbeis, *Chem. Eur. J.*, 1998, **4**, 1810.

21 (*a*) A. P. de Silva, H. Q. N. Gunaratne and C. P. McCoy, *Chem. Commun.*, 1996, 2399; (*b*) L. Fabbrizzi, F. Gatti, P. Pallavicini and L. Parodi, *New J. Chem.*, 1998, **22**, 1403; (*c*) L. Fabbrizzi, M. Licchelli, L. Parodi, A. Poggi and A. Taglietti, *Eur. J. Inorg. Chem.*, 1999, 35.

22 D. M. Jordan, D. R. Walt and F. P. Milanovich, *Anal. Chem.*, 1987, **59**, 437.

23 (*a*) H. E. Posch, M. J. P. Leiner and O. S. Wolfbeis, *Fresenius J. Anal. Chem.*, 1989, **334**, 162; (*b*) D. R. Walt, G. Gabor and C. Goyet, *Anal. Chim. Acta*, 1993, **274**, 47; (*c*) J. R. Lakowicz, H. Szmacinski and M. Karakelle, *Anal. Chim. Acta*, 1993, **272**, 179.

24 A. P. de Silva, H. Q. N. Gunaratne, T. Gunnlaugsson and P. L. M. Lynch, *New J. Chem.*, 1996, **20**, 871.

25 (*a*) F. Pina, M. J. Melo, M. A. Bernardo, S. V. Luis and E. García-España, *J. Photochem. Photobiol. A*, 1999, **126**, 65; (*b*) J. Ji and Z. Rosenzweig, *Anal. Chim. Acta*, 1999, **397**, 93.

26 (*a*) A. P. de Silva, H. Q. N. Gunaratne and C. P. McCoy, *Nature (London)*, 1993, **364**, 42; (*b*) A. P. de Silva, H. Q. N. Gunaratne and C. P. McCoy, *J. Am. Chem. Soc.*, 1997, **119**, 7891; (*c*) A. P. de Silva, I. M. Dixon, H. Q. N. Gunaratne, T. Gunnlaugsson, P. R. S. Maxwell and T. E. Rice, *J. Am. Chem. Soc.*, 1999, **121**, 1393.

27 (*a*) M. Vignes, E. Blanc, J. Guiramand, E. Gonzalez, I. Sassetti and M. Recasens, *Neuropharmacology*, 1996, **35**, 1595; (*b*) S. D'Souza, A. Garcia-Cabado, F. Yu, K. Teter, G. Lukacs, K. Skorecki, H.-P. Moore, J. Orlowski and S. Grinstein, *J. Biol. Chem.*, 1998, **273**, 2035; (*c*) J. M. Salvador, G. Inesi, J.-L. Rigaud and A. M. Mata, *J. Biol. Chem.*, 1998, **273**, 18230.

28 (*a*) G. R. Martin and R. K. Jain, *Microvasc. Res.*, 1993, **46**, 216; (*b*) T. B. Wiegmann, L. W. Welling, D. M. Beatty, D. E. Howard, S. Vamos and S. J. Morris, *Am. J. Physiol.*, 1993, **265**, C1184; (*c*) Y. Kostov and G. Rao, *Rev. Sci. Instrum.*, 1999, **70**, 4466.

29 A. I. Harianawala and R. H. Bogner, *J. Lumin.*, 1998, **79**, 97.

30 (*a*) L. A. Saari and W. R. Seitz, *Anal. Chem.*, 1982, **54**, 821; (*b*) M. L. Graber, D. C. DiLillo, B. L. Friedman and E. Pastoriza-Munoz, *Anal. Biochem.*, 1986, **156**, 202; (*c*) J. Liu, Z. Diwu and D. H. Klaubert, *Bioorg. Med. Chem. Lett.*, 1997, **7**, 3069; (*d*) A. Elamari, N. Gisin, H. Zbinden, J. L. Munoz, S. Poitry and M. Tsacopoulos, *Sens. Actuators B*, 1997, **38**, 39, 183.

31 (*a*) R. B. Robey, O. Ruiz, A. V. P. Santos, J. Ma, F. Kear, L.-J. Wang, C.-J. Li, A. A. Bernardo and J. A. L. Arruda, *Biochemistry*, 1998, **37**, 9894; (*b*) M. Kneen, J. Farinas, Y. Li and A. S. Verkman, *Biophys. J.*, 1998, **74**, 1591.

32 R. B. Thompson and J. R. Lakowicz, *Anal. Chem.*, 1993, **65**, 853.

33 (*a*) D. W. Lübbers and N. Opitz, *Z. Naturforsch., Teil C*, 1975, **30**, 532; (*b*) Z. Zhujun and W. R. Seitz, *Anal. Chim. Acta*, 1984, **160**, 305; (*c*) C. Munkholm and D. R. Walt, *Talanta*, 1988, **35**, 109.

34 (*a*) R. Y. Tsien and M. Poenie, *Trends Biochem. Sci.*, 1986, **11**, 450; (*b*) G. R. Bright, G. W. Fisher, J. Rogowska and D. L. Taylor, *J. Cell Biol.*, 1987, **104**, 1019; (*c*) G. R. Bright, G. W. Fischer, J. Rogowska and D. L. Taylor, *Methods Cell Biol.*, 1989, **30**, 157; (*d*) R. B. Silver, *Methods Cell Biol.*, 1998, **56**, 237.

35 (*a*) S. Bassnett, L. Reinisch and D. C. Beebe, *Am. J. Physiol.*, 1990, **258**, C171; (*b*) J. F. Whitaker, R. P. Haugland and F. G. Prendergast, *Anal. Biochem.*, 1991, **194**, 330.

36 A. Bromberg, J. Zilberstein, G. Frishman, S. Riesemberg, E. Benori, E. Silberstein, J. Zimnavoda and A. Kritzman, *Sens. Actuators B*, 1996, **31**, 181.

37 H. Chao, B.-H. Ye, Q.-L. Zhang and L.-N. Ji, *Inorg. Chem. Commun.*, 1999, **2**, 338.

38 T. Werner, I. Klimant and O. S. Wolfbeis, *J. Fluoresc.*, 1994, **4**, 41.
39 M. Kuratli and E. Pretsch, *Anal. Chem.*, 1994, **66**, 85.
40 T. Werner and O. S. Wolfbeis, *Fresenius J. Anal. Chem.*, 1993, **346**, 564.
41 C. Müller, B. Hitzmann, T. Scheper and F. Schubert, *Sens. Actuators B*, 1997, **40**, 71.
42 R. Y. Tsien, *Annu. Rev. Neurosci.*, 1989, **12**, 227; *Intracellular pH and its Measurement*, eds. A. Kotyk and J. Slavik, CRC, Boca Raton, FL, 1994; J. Slavik, *J. Lumin.*, 1997, **72–74**, 575.
43 J. N. Moorthy, T. Shevchenko, A. Magon and C. Bohne, *J. Photochem. Photobiol.*, A, 1998, **113**, 189.
44 T. Kobayashi, T. Fukaya and N. Fujii, *J. Membr. Sci.*, 2000, **164**, 157.
45 R. S. Pomeroy, M. E. Baker, M. B. Denton and A. G. Dickson, *Appl. Spectrosc.*, 1995, **49**, 1729.
46 (*a*) F. Deng and A. C. Testa, *J. Photochem. Photobiol. A*, 1998, **112**, 191; (*b*) F. Deng, J. Kubin and A. C. Testa, *J. Photochem. Photobiol.*, A, 1998, **118**, 1.
47 S. G. Schulman, in *Modern Fluorescence Spectroscopy*, ed. E. L. Wehry, Heyden & Son, London, 1976, vol. 2, p. 239; H. Inoue, M. Hida, N. Nakashima and K. Yoshiharo, *J. Phys. Chem.*, 1982, **86**, 3184; J. Konijnenberg, G. B. Ekelmans, A. H. Huizer and C. A. G. O. Varma, *J. Chem. Soc., Faraday Trans. 2*, 1989, **85**, 39; R. Das, S. Mitra and S. Mukherjee, *Chem. Phys. Lett.*, 1994, **221**, 368; S. I. Druzhinin, B. D. Bursulaya and B. M. Uzhinov, *J. Photochem. Photobiol. A*, 1995, **90**, 53.
48 (*a*) N. Ikeda, H. Miyasaka, T. Okada and N. Mataga, *J. Am. Chem. Soc.*, 1983, **105**, 5206; (*b*) C. Cazeau-Dubroca, A. Peirigua, M. B. Brahim, G. Nouchi and P. Cazeau, *Chem. Phys. Lett.*, 1989, **157**, 393; (*c*) T. López Arbeloa, F. López Arbeloa, P. Hernández Bartolomé and I. López Arbeloa, *Chem. Phys.*, 1992, **160**, 123; (*d*) J. Herbich and J. Waluk, *Chem. Phys.*, 1994, **188**, 247; (*e*) A. Kadiri, B. Kabouchi, B. Benali, C. Cazeau-Dubroca and G. Nouchi, *Spectrochim. Acta, Part A*, 1994, **50**, 1; (*f*) T. López Arbeloa, F. López Arbeloa and I. López Arbeloa, *J. Luminesc.*, 1996, **68**, 149; (*g*) E. Martin, E. Weigand and A. Pardo, *J. Luminesc.*, 1996, **68**, 157; (*h*) Y. H. Kim, D. W. Cho, N. W. Song, D. Kim and M. Yoon, *J. Photochem. Photobiol. A*, 1997, **106**, 161.
49 (*a*) M. Kollmannsberger, K. Rurack, U. Resch-Genger and J. Daub, *J. Phys. Chem. A*, 1998, **102**, 10211; (*b*) K. Rurack, M. Kollmannsberger, U. Resch-Genger and J. Daub, *J. Am. Chem. Soc.*, 2000, **122**, 968.
50 K. Rurack, W. Rettig and U. Resch-Genger, *Chem. Commun.*, 2000, 407; K. Rurack, J. L. Bricks, B. Schulz, M. Maus, G. Reck and U. Resch-Genger, *J. Phys. Chem. A*, 2000, **104**, 6171.
51 W. Rettig, *Angew. Chem., Int. Ed. Engl.*, 1986, **25**, 971.
52 M. Maus, W. Rettig, D. Bonafoux and R. Lapouyade, *J. Phys. Chem. A*, 1999, **103**, 3388.
53 (*a*) M. Maus, W. Rettig and R. Lapouyade, *J. Inf. Rec.*, 1996, **22**, 451; (*b*) W. Rettig and M. Maus, *Ber. Bunsen-Ges. Phys. Chem.*, 1996, **100**, 2091; (*c*) M. Maus and W. Rettig, *J. Inf. Rec.*, 1998, **24**, 461.
54 H. Shizuka, *Acc. Chem. Res.*, 1985, **18**, 141.
55 (*a*) J. Dey and S. K. Dogra, *J. Phys. Chem.*, 1994, **98**, 3638; (*b*) G. Krishnamoorthy and S. K. Dogra, *Chem. Phys.*, 1999, **243**, 45.
56 (*a*) T. Gareis, C. Huber, O. S. Wolfbeis and J. Daub, *Chem. Commun.*, 1997, 1717; (*b*) T. Werner, C. Huber, S. Heinl, M. Kollmannsberger, J. Daub and O. S. Wolfbeis, *Fresenius J. Anal. Chem.*, 1997, **359**, 150.
57 D. Piorun, A. B. J. Parusel, K. Rechthaler, K. Rotkiewicz and G. Köhler, *J. Photochem. Photobiol. A*, 1999, **129**, 33.
58 G. E. Collins, L.-S. Choi and J. H. Callahan, *J. Am. Chem. Soc.*, 1998, **120**, 1474.
59 M. Maus, *Photoinduced Intramolecular Charge Transfer in Donor–Acceptor Biaryls and Resulting Applicational Aspects*, Dissertation.com, Parkland, FL, 1998.
60 M. Maus, W. Rettig, G. Jonusauskas, R. Lapouyade and C. Rullière, *J. Phys. Chem. A*, 1998, **102**, 7393.
61 (*a*) T. Förster, *Z. Elektrochem. Angew. Phys. Chem.*, 1950, **54**, 42; (*b*) E. Lippert, *Organic Molecular Photophysics*, ed. J. B. Birks, Wiley & Sons, London, 1975.
62 S. Hagopian and A. Singer, *J. Am. Chem. Soc.*, 1985, **107**, 1874.
63 E. L. Wehry, *in Practical Fluorescence*, ed. G. G. Guilbault, Marcel Dekker, New York, 1990, p. 127.
64 H. Shizuka, T. Ogiwara and E. Kimura, *J. Phys. Chem.*, 1985, **89**, 4302.
65 S. A. Jonker, F. Ariese and J. W. Verhoeven, *Recl. Trav. Chim. Pays-Bas*, 1989, **108**, 109.
66 J. Saciv, A. Yogev and Y. Mazur, *J. Am. Chem. Soc.*, 1977, **99**, 6861.
67 Y. Zhu and G. B. Schuster, *J. Am. Chem. Soc.*, 1990, **112**, 8583.
68 C. David and D. Baeyens-Volant, *Mol. Cryst. Liq. Cryst.*, 1980, **59**, 181.
69 M. Maus and W. Rettig, *Chem. Phys.*, 1997, **218**, 151.
70 (*a*) J. Herbich and A. Kapturkiewicz, *J. Am. Chem. Soc.*, 1998, **120**, 1014; (*b*) A. Kapturkiewicz, J. Herbich, J. Karpiuk and J. Nowacki, *J. Phys. Chem. A*, 1997, **101**, 2332.
71 M. Maus and W. Rettig, *Chem. Phys.*, in press.
72 W. Rettig, V. Kharlanov and M. Maus, *Chem. Phys. Lett.*, 2000, **318**, 173.
73 (*a*) P. Fromherz, *J. Phys. Chem.*, 1991, **95**, 6792; (*b*) P. Fromherz and A. Heilemann, *J. Phys. Chem.*, 1992, **96**, 6864.
74 R. A. Velapoldi, in *Advances in Standards and Methodology in Spectrophotometry*, eds. C. Burgess and K. D. Mielenz, Elsevier Science, Amsterdam, 1987, p. 175.
75 C. A. Parker, *Photoluminescence of Solutions*, Elsevier, Amsterdam, 1968.
76 R. A. Velapoldi and M. S. Epstein, in *Luminescence Applications in Biological, Chemical, Environmental and Hydrological Sciences*, ed. M. C. Goldberg, American Chemical Society, Washington, DC, 1989, vol. 383, p. 98.
77 J. A. Riddick, W. B. Bunger and T. K. Sakano, *Organic Solvents*, John Wiley & Sons, New York, 1986.
78 H. Galster, *pH-Messung*, VCH Verlagsgesellschaft, Weinheim, 1990.
79 (*a*) D. Parker, K. Senanayake and J. A. G. Williams, *Chem. Commun.*, 1997, 1777; (*b*) D. Parker and J. A. G. Williams, *Chem. Commun.*, 1998, 245; (*c*) T. Gunnlaugsson and D. Parker, *Chem. Commun.*, 1998, 511; (*d*) D. Parker, P. K. Senanayake and J. A. G. Williams, *J. Chem. Soc., Perkin Trans. 2*, 1998, 2129.
80 (*a*) R. Grigg and N. D. J. A. Norbert, *J. Chem. Soc. Chem. Commun.*, 1992, 1300; (*b*) F. Barigelletti, L. Flamigni, M. Guardigli, J.-P. Sauvage, J.-P. Collin and A. Sour, *Chem. Commun.*, 1996, 1329; (*c*) A. M. W. Cargill Thompson, M. C. C. Smailes, J. C. Jeffery and M. D. Ward, *J. Chem. Soc., Dalton Trans.*, 1997, 737; (*d*) B. Jing, A. Song, M. Zhang and T. Shen, *Chem. Lett.*, 1999, 789.
81 A. Declémy, C. Rulière and P. Kottis, *Laser Chem.*, 1990, **10**, 413.
82 J. R. Platt, *J. Chem. Phys.*, 1949, **17**, 484.